Journal of Dynamic Behavior of Materials (2019) 5:51–58
https://doi.org/10.1007/s40870-019-00183-1

Energy Dissipation Characteristics in Pre-strained Silicone Foam Transitioning to Silicone Rubber

Brett Sanborn[1] · **Bo Song**[1]

Received: 22 October 2018 / Accepted: 11 January 2019 / Published online: 25 February 2019

Abstract
Silicone foam is used as a shock mitigation material in a variety of systems to protect internal components from being damaged during external shock or impact loading. Characterizing the shock mitigation response of silicone foam under a variety of scenarios is a critical step in designing and/or evaluating new shock mitigation systems. In this study, a Kolsky bar with pre-compression capability was used with a passive radial confinement tube to subject the sample to various levels of pre-strain followed by impact loading. The effects of both pre-strain and impact velocity on impact energy dissipation behavior were investigated for silicone foam. The energy dissipation response of silicone foam is compared to a silicone rubber manufactured using the same processing methods to understand the energy dissipation characteristics of silicone foams transitioning to a silicone rubber. The final density of the foam or rubber plays a key role in both the total energy dissipation ratio in the time domain and the energy dissipation ratio as a function of frequency in the frequency domain.

Keywords Kolsky bar · Frequency response · Silicone foam · Silicone rubber · Energy dissipation · Shock mitigation

Introduction

In addition to high-g acceleration, high frequency is a key factor that can cause potential damage to internal electronics in scenarios ranging from portable electronics to defense applications [1, 2]. Selection of a shock mitigation material is typically dictated by the ability of the material to dissipate impact energy in total or over a range of frequencies for a specific application. Rubbers in both the solid and foamed state have been extensively utilized as shock mitigation materials [3–5]. Silicone rubber and foams are examples that are used in shock mitigation designs for different external loading environments. Depending on the configuration, silicone rubber or foam may be subjected to different stress-states, strain rates, and temperatures, all of which could change the shock mitigation behavior. Compared to dense silicone rubber, silicone foam is less stiff and much more compressible, and may also be pre-strained in compression during the installation and assembly process. Due to low stiffness and nonlinear stress–strain response [6, 7], the silicone foam may exhibit completely different shock mitigation performance when pre-strained. Furthermore, the shock mitigation performance of silicone foam may also depend on the level of pre-strain. If silicone foam is subjected to a relatively large pre-strain, the material may become densified and behave like a nearly incompressible silicone rubber. A transition in Poisson's ratio from 0.22 to 0.47 in a silicone foam with ~50% porosity has been observed to occur at roughly 0.5 engineering strain, which is considered to be the densification strain [8]. Such a drastic change in densification state could significantly change the impact energy dissipation capability in both the time and the frequency domains. The relationship between densification state and impact energy dissipation for foam material is yet unstudied. Therefore, experimental and analytical investigation of the shock mitigation response of both silicone foam and rubber in assembly-like mechanical environments is required to improve design and specify installation/assembly procedures in vibration control and shock-resistant packaging.

The overall energy absorption capacity of a foam material is usually evaluated with the maximum absorbed energy per volume prior to densification [9]. While total energy

Mr. Brett Sanborn and Dr. Bo Song are the members of the Society for Experimental Mechanics.

✉ Brett Sanborn
bsanbor@sandia.gov

[1] Sandia National Laboratories, PO Box 5800, MS0557, Albuquerque, NM 87185, USA

absorption capacity of the material is important, the energy absorption capabilities of foam materials may be frequency dependent, meaning that foam materials may absorb different amounts of energy at different frequencies. Few studies have investigated the frequency-domain energy dissipation behavior of materials under impact loading. Frequency-domain energy dissipation for unconfined polymethylene diisocyanate (PMDI) based rigid polyurethane foam using a Kolsky compression bar was first investigated by Song and Nelson [10]. Their results showed that the PMDI foam had a characteristic energy dissipation cutoff frequency of 1.5 kHz. Recently, Sanborn et al. [11] studied the frequency domain energy dissipation properties of a confined silicone foam using a similar Kolsky compression bar setup. In that study, passively confined silicone foam was subjected to increasing levels of quasi-statically applied pre-strain before impact loading using a Kolsky compression bar. Sanborn et al. [11] showed that up to 33.5% pre-strain, the silicone foam dissipated more than 99% of the impact energy over the frequency range. The cutoff frequency of the silicone foam was observed to decrease from 2.65 kHz to 2 kHz when the pre-strain decreased from 23.3 to 13%. However, only one impact velocity was investigated in that study, and the silicone foam may dissipate impact energy differently at different loading speeds and higher amounts of pre-strain due to significant nonlinear stress–strain behavior and strain-rate effects [11]. Therefore, the effect of impact speed on energy dissipation needs to be investigated.

Changing the impact speed may not only induce a strain rate effect in the material but may also affect the densification state of the foam. For a constant loading duration, a higher impact speed generates higher specimen strain and results in higher density of the foam material under investigation. The increased foam density may totally change the shock mitigation capacity, particularly when the foam material is densified to an incompressible state. In addition, adding pre-strain to the silicone foam material prior to dynamic loading further increases the final density. The final density could be an important parameter to investigate the transitional characteristic of impact energy dissipation from compressible foam materials to fully dense and nearly incompressible rubber. The effect of final density caused by impact speed and/or pre-strain on impact energy dissipation for foam materials has not yet been fully investigated.

In this study, we followed a similar procedure presented in an earlier work [11] to investigate the shock mitigation behavior of pre-strained silicone foams and un-pre-strained silicone rubber to understand the effect of impact speed on energy dissipation. The energy dissipation behavior of silicone foam is compared to a solid silicone rubber that comprises the foam matrix to reveal the difference of impact energy dissipation characteristics between solid and foamed materials. The data are also used to determine the effect of final density on impact energy dissipation during the transition process from a foam to a solid rubber material.

Specimens and Experimental Setup

The silicone foam and silicone rubber under investigation were processed using the same chemistry; however, in the case of silicone foam, plastic pellets were introduced into the mixture during processing to give the material porosity and were subsequently removed using a wash-out process. This addition and removal of pellets to the processing resulted in an average cell size in the material of approximately 0.5 mm (Fig. 1a). The pellet mixture was not added to one batch during processing which resulted in a solid silicone rubber (Fig. 1b). Comparing the density of the two materials, the open-cell silicone foam had a non-compressed density of

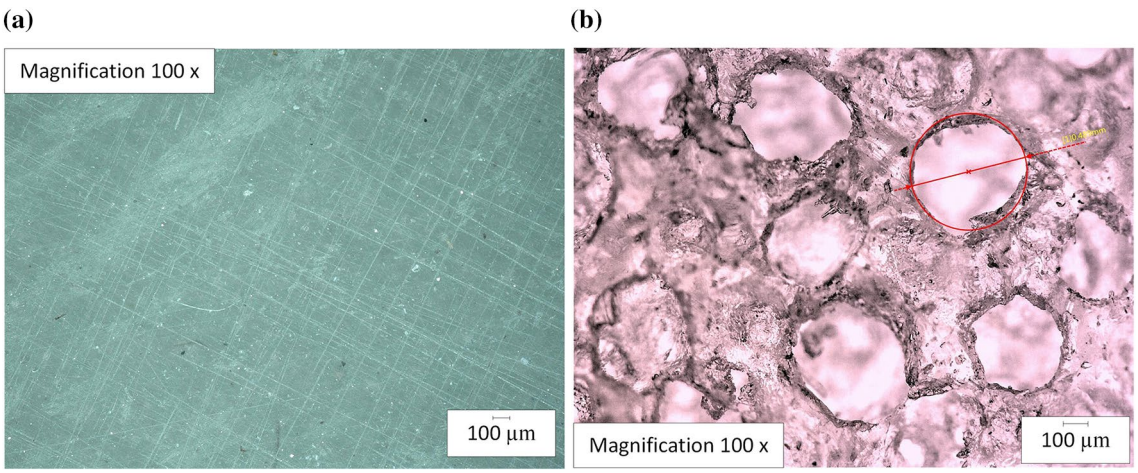

Fig. 1 Optical micrograph of **a** silicone foam and **b** silicone rubber

608 ± 21.85 kg/m^3 while the silicone rubber had a density of 1153 kg/m^3. More accurately, both the silicone foam and silicone rubber were made of the same silicone rubber, but in the different forms: foamed and solid. Silicone foam can be more accurately termed "silicone rubber foam," but "silicone foam" is used throughout the paper for brevity.

In this study, the silicone foam was subjected to pre-strains of 0, 13, 23.3 and 33.5% in compression prior to dynamic compressive loading while the silicone rubber was subjected to a non-pre-strained condition. The specimen information, pre-strain level, and impact speed are detailed in Table 1.

A Kolsky bar with pre-load capability as discussed in [11] was used to apply dynamic loading to the specimens. To briefly summarize, the Kolsky bar setup, as shown in Fig. 2, used a tapered tungsten striker which impacted the end of the incident bar and created a loading pulse that propagated along the incident bar to load the specimen sandwiched between the incident and transmission bars. The tungsten striker was used to apply a wide range of frequencies to the sample [11, 12]. The specimen was confined in a steel tube that had an inner diameter the same as the specimen diameter. This design and configuration provided passive confinement such that the specimen was deformed in a nearly one-dimensional strain state which is close to the state experienced by the silicone foam/rubber in real shock mitigation applications. In addition, to simulate the possible static pre-compression subjected to the silicone foam/rubber during the assembly process, a variety of pre-strain levels were quasi-statically applied to the specimen prior to impact loading. A linear laser and detector system, which was used for specimen displacement measurement in Kolsky tension bar experiments, was slightly modified to measure the amount of engineering pre-strain quasi-statically applied to the specimens (Fig. 2) [11, 13]. More experimental setup details have been presented in reference [11].

The Kolsky compression bar tests followed the standard data acquisition procedure using strain gages. After the incident (ε_i), reflected (ε_r) and transmitted (ε_t) pulses are acquired, the incident (E_i), reflected (E_r), and transmitted (E_t) energies can be calculated [10, 14, 15]

$$E_i(t) = A_0 C_0 E_0 \int_0^t \varepsilon_i(t)^2 dt \tag{1}$$

$$E_r(t) = A_0 C_0 E_0 \int_0^t \varepsilon_r(t)^2 dt \tag{2}$$

$$E_t(t) = A_0 C_0 E_0 \int_0^t \varepsilon_t(t)^2 dt \tag{3}$$

where A_0 is the cross-sectional area of the pressure bars; C_0 and E_0 are one-dimensional elastic wave speed and Young's modulus of the bar material. In this study, the incident and transmission bars were made of the same material (maraging C300 steel) and had a common diameter of 25.4 mm. The total absolute dissipated energy (Δ) and energy dissipation ratio (δ) in the specimen over the duration of loading (T) are calculated as [10]

$$\Delta = E_i(t) - E_r(t) - E_t(t) = A_0 C_0 E_0 \int_0^T \left[\varepsilon_i(t)^2 - \varepsilon_r(t)^2 - \varepsilon_t(t)^2\right] dt \tag{4}$$

$$\delta = \frac{\Delta(t)}{E_i(t) - E_r(t)} = \frac{\int_0^T \left[\varepsilon_i(t)^2 - \varepsilon_r(t)^2 - \varepsilon_t(t)^2\right] dt}{\int_0^T \left[\varepsilon_i(t)^2 - \varepsilon_r(t)^2\right] dt} \tag{5}$$

Table 1 Materials and specimen geometries

Material	Initial density (kg/m^3)	Diameter (mm)	Thickness (mm)	Applied pre-strain (%)	Impact speed (m/s)
Silicone foam	608 ± 21.85	25.37 ± 0.08	5.25	0, 13, 23.3, 33.5	5.6, 12.8
Silicone rubber	1153	25.37 ± 0.08	1.93	0	5.6, 12.8, 22.4

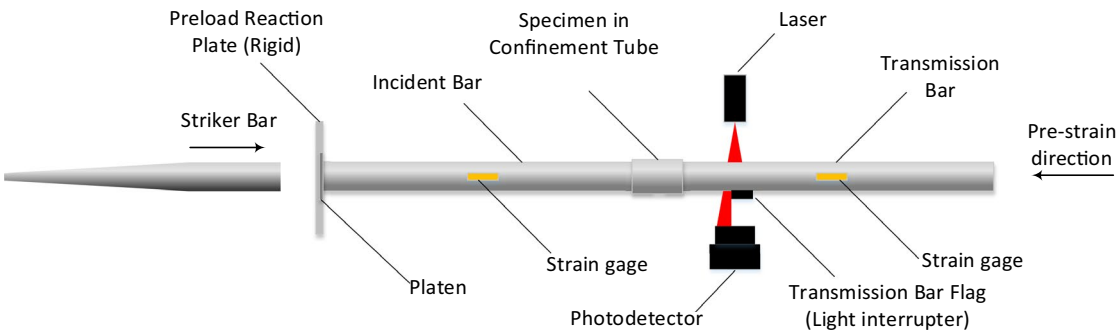

Fig. 2 Kolsky compression bar for passive confinement frequency-based silicone foam and rubber experiments

In the frequency domain, the incident (S_i), reflected (S_r), and transmitted (S_t) energy spectrum density are [10, 11]

$$S_i(f) = A_0 C_0 E_0 \left|B_i(f)\right|^2 \tag{6}$$

$$S_r(f) = A_0 C_0 E_0 \left|B_r(f)\right|^2 \tag{7}$$

$$S_t(f) = A_0 C_0 E_0 \left|B_t(f)\right|^2 \tag{8}$$

where $B_i(f)$, $B_r(f)$, and $B_t(f)$ are the magnitudes of the Fourier transforms of the incident, reflected, and transmitted pulses, respectively. The energy dissipation ratio as a function of frequency is thus computed as [10, 11]

$$d(f) = 1 - \frac{\left|B_t(f)\right|^2}{\left|B_i(f)\right|^2 - \left|B_r(f)\right|^2} \tag{9}$$

Results and Discussion

The incident and transmission bar strain gage histories from a typical experiment on the silicone foam are shown in Fig. 3a. As shown in Fig. 3a, the transmission bar strain was approximately 600 times lower than the incident bar strain due to the very soft silicone foam specimen. Therefore, a pair of semiconductor strain gages with approximately 80 times higher sensitivity than the foil resistive strain gages on the incident bar were used to record the weak transmitted signal with high resolution. Figure 3b. shows a typical signal recorded from an experiment on the silicone rubber using the same input conditions as Fig. 3a. Unlike for silicone foam experiments (Fig. 3a), the semiconductor strain gages were not required for the silicone rubber experiments due to a higher transmission signal which was on the same order as the incident signal. This indicates that the silicone rubber is difficult to compress when radially confined, meaning that most of the impact energy was transferred through the material into the transmission bar.

The stress-time histories of the silicone foam subjected to the four different pre-strain levels at the same impact speed (12.8 m/s) are shown in Fig. 4. The maximum stress at 33.5% pre-strain was about 300 times higher than the maximum stress measured under the same impact conditions for 0 and 13% pre-strain (Fig. 4b). This is because the foam specimens were deformed to higher total strains when they were subjected to higher (quasi-static) pre-strain levels. The strain rates were also higher due to smaller initial thickness in the foam specimens subjected to higher pre-strain levels even though the impact speed was the same. The response at each of the pre-strains was repeatable with slight differences in the amount of peak stress recorded, as shown in Fig. 4.

The stress-time histories for confined, non-pre-strained silicone rubber are shown in Fig. 5 at three different impact velocities. With increasing impact velocity, the stress amplitude in the silicone rubber significantly increased. The shape of the stress history of silicone rubber is like that of silicone foam, but the stress amplitudes of the silicone rubber were higher than those of the silicone foam. Furthermore, the peak stress observed for silicone rubber at the lowest speed (5.6 m/s) is close to the stress history of silicone foam pre-strained to 33.5% impacted at 12.8 m/s. This suggests that the silicone foam pre-strained to 33.5% subjected to a higher impact velocity may have reached a similar state of densification perhaps approaching the solid silicone rubber.

The incident, reflected, and transmitted strains in the pressure bars were used with Eqs. 5 and 6 to calculate the total dissipated energy through the pre-strained silicone foams and non-pre-strained silicone rubber at different impact velocities.

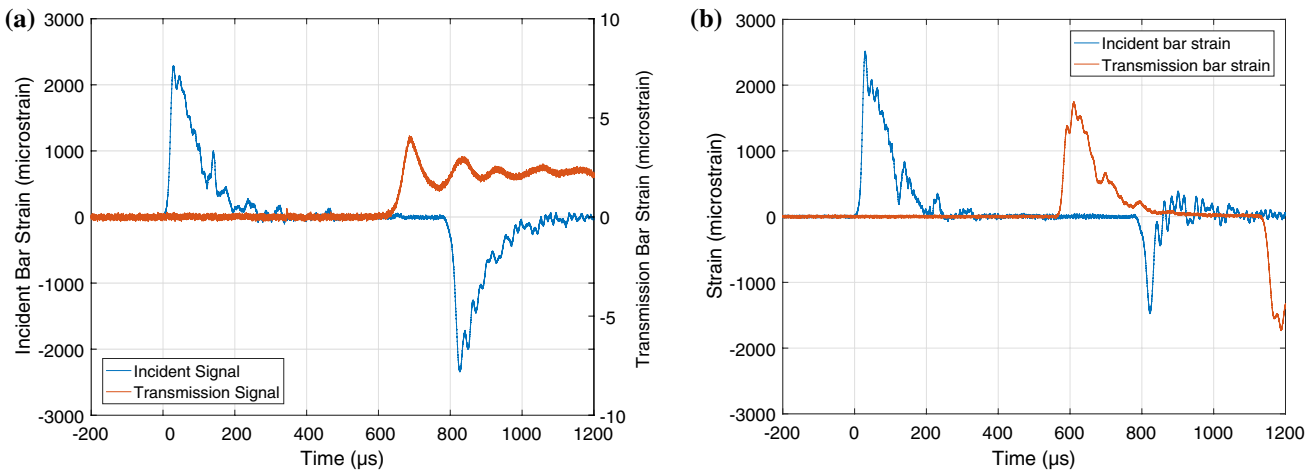

Fig. 3 Original records from experiments on confined **a** non-compressed silicone foam and **b** non-compressed silicone rubber using the same impact speed of 12.8 m/s

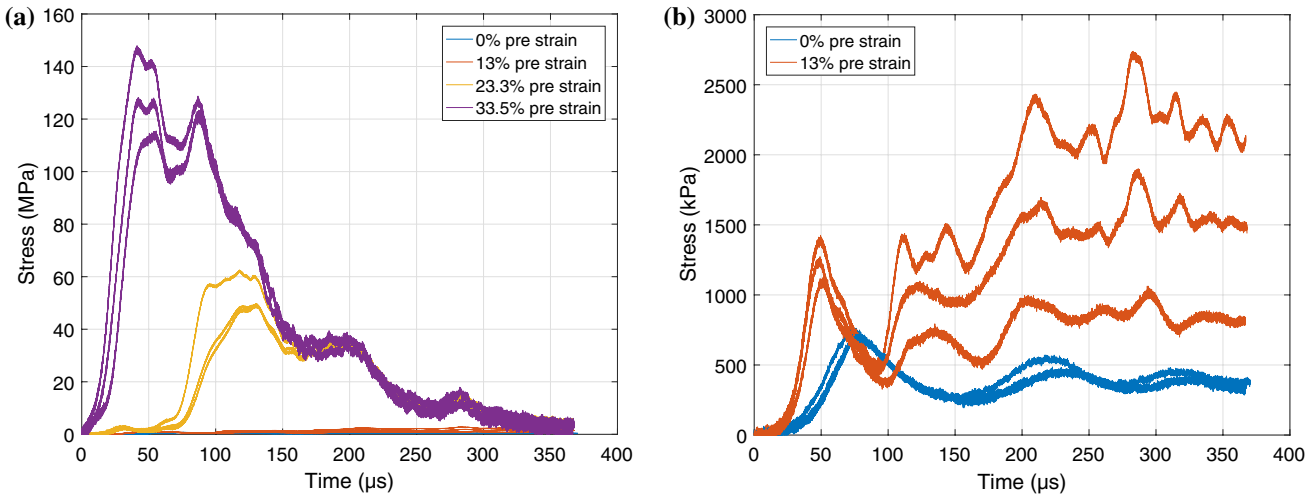

Fig. 4 **a** Stress-time histories of the confined silicone foam at various pre-strains. Note that stress levels for 0 and 13% pre-strains are orders of magnitude lower than 23.3 and 33.5% pre-strains. **b** Stress-time histories of the confined silicone foam at low pre-strain levels

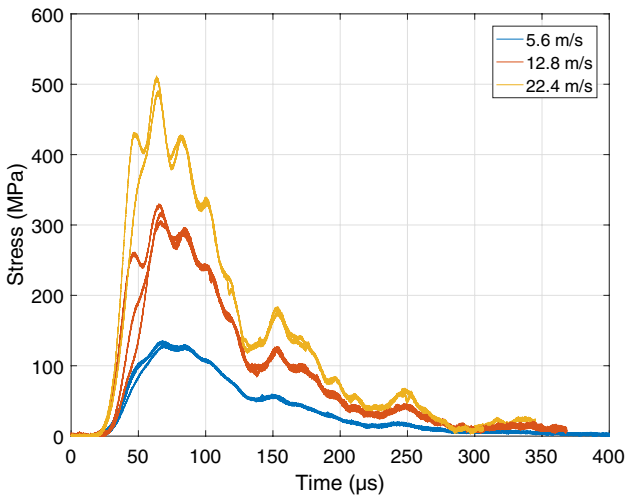

Fig. 5 Stress-time histories for silicone rubber at three different impact velocities

The calculation results are summarized in Table 2. Table 2 also contains values of specific energy dissipated by the foam based upon the initial volume of the foam specimens. As shown in both Table 2, for the silicone foam, there is no difference in the energy dissipation ratios for the silicone foams pre-strained to 0 and 13.3% which are close to 1 and independent of impact velocity. This means the silicone foam exhibited superior energy dissipation capability when not or only slightly pre-strained. This could indicate that the silicone foam might not be fully densified during impact loading at those pre-strain levels. With increasing pre-strain, the energy dissipation ratio of the silicone foam decreased, particularly at the higher impact velocity of 12.8 m/s. A reason for this could be that at a higher impact velocity and a larger pre-strain, the silicone foam may become fully densified and act as a nearly incompressible silicone rubber, which would significantly reduce the energy dissipation capacity. The high rate, unconfined compressive stress–strain behavior of the same silicone foam material indicates that densification begins at roughly 50% engineering strain [8] indicated by a sharp upturn in the stress–strain response. Similarly, the Poisson's ratio of silicone foam transitions from compressible to nearly incompressible after being densified [8]. While the confined response is most likely different, especially in terms of the Poisson's ratio, the material may densify at a similar strain level whenever cell collapse occurs. This assumption can be tested by looking at the energy dissipation ratio for the silicone rubber, also shown in Table 2. The silicone rubber exhibited only 25% energy dissipation ratio independent of impact velocity. Hence, the silicone foam may reach this apparent lower limit of energy dissipation of the silicone rubber if compressed beyond the densification strain.

Since the densification state of silicone foams appears to be an important parameter with regards to energy dissipation capability, the densification state can be described as a final density of the material after impact loading. After impact, the total specimen strain becomes

$$\varepsilon_{total} = \varepsilon_{pre} + \varepsilon_{dynamic} \tag{11}$$

where ε_{pre} is the pre-strain applied to the specimen prior to dynamic loading, $\varepsilon_{dynamic}$ is strain generated in the specimen during dynamic loading, which is calculated with [16]

$$\varepsilon_{dynamic} = -\frac{C_0}{L_s}\int_o^t \left(\varepsilon_i - \varepsilon_r - \varepsilon_t\right)dt \tag{12}$$

Table 2 Energy dissipated by silicone foam and rubber under different conditions

Impact speed (m/s)	Applied pre-strain (%)	Total engineering strain (%)	Input energy (J)	Specific energy (J/cc)	Average energy dissipation ratio
Foam					
5.6	0	15.8 ± 0.13	1.04 ± 0.27	0.38 ± 0.10	0.9999
5.6	13	28.8 ± 0.12	1.64 ± 0.21	0.70 ± 0.09	0.9999
5.6	23.3	39.1 ± 0.18	1.49 ± 0.69	0.72 ± 0.34	0.9996
5.6	33.5	48.8 ± 0.11	1.77 ± 0.25	0.99 ± 0.14	0.9943
12.8	0	37.2 ± 0.01	18.99 ± 2.49	7.16 ± 0.94	0.9999
12.8	13	50.1 ± 0.28	21.49 ± 2.78	9.31 ± 1.20	0.9996
12.8	23.3	54.3 ± 0.71	24.13 ± 1.05	11.85 ± 0.52	0.8466
12.8	33.5	55.3 ± 1.17	41.69 ± 0.56	23.62 ± 0.77	0.5865
Rubber					
5.6	0	12.0 ± 0.73	20.42 ± 0.56	20.93 ± 0.57	0.2563
12.8	0	24.5 ± 4.22	103.86 ± 9.95	106.45 ± 10.19	0.2735
22.4	0	30.4 ± 3.22	225.20 ± 1.84	230.82 ± 1.89	0.2570

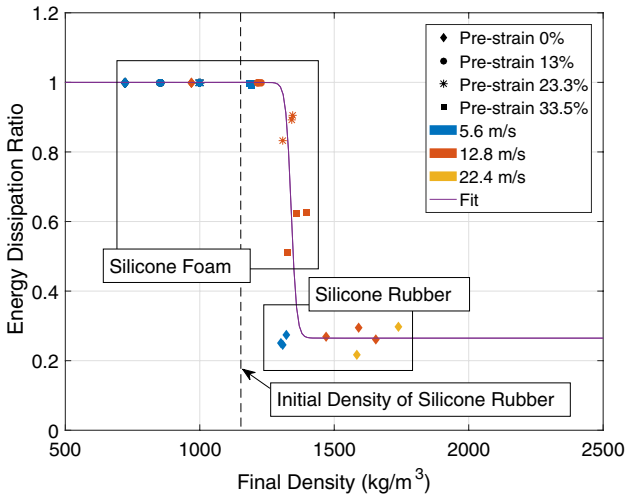

Fig. 6 Relationship between total energy dissipation ratio in the frequency-domain and final density of the specimen

where L_s is the specimen length. Since the specimen is constrained by the confinement tube, the specimen diameter remained constant throughout the experiment. Knowing the initial density, the final density was calculated using the dimensions of the deformed volume, which simplifies to

$$\rho_{final} = \frac{\rho_{initial}}{(1 - \varepsilon_{total})} \tag{13}$$

Figure 6 shows the relationship between energy dissipation ratio and final density of both silicone foam and rubber. The initial density of silicone rubber (1153 kg/m^3) is also presented as a dashed line in Fig. 6. As shown in Fig. 6, there appears to be a critical density between 1200 and 1400 kg/m^3 (slightly higher than the initial density of solid silicone rubber), at which the energy dissipation ratio drastically changes. When the final density of silicone foam was lower than the critical density, the silicone foam exhibited superior energy dissipation capability: nearly all input energy was dissipated. However, when the final density of silicone foam was higher than the critical density, the energy dissipation ratio of the silicone foam significantly dropped to approximately 0.6 and approached 0.25, which is the energy dissipation ratio for silicone rubber, as indicated with the solid 'Fit' line in Fig. 6. This indicates that there is a transitional process of energy dissipation from the silicone foam to silicone rubber. In addition, the energy dissipation ratio for the silicone rubber depends on neither final density nor impact velocity within the range conducted in this study.

Using the strain–time histories of the incident, reflected, and transmitted pulses and Eqs. 6–9, the energy dissipation ratios as a function of frequency for all experiments were calculated. Figure 7 shows typical frequency-domain energy dissipation ratio behavior for the silicone foam pre-strained to 33.5% at two impact velocities: 5.6 and 12.8 m/s. At each condition, three experiments were repeated. Due to discontinuities in frequency spectrum, the energy dissipation ratio was investigated in the frequency domain up to 10 kHz. At the lower impact velocity (5.6 m/s), the pre-strained silicone foam exhibited a high energy dissipation ratio (0.99) at frequencies up to 400 Hz. However, at the higher impact velocity (12.8 m/s), about 80% of energy was dissipated at frequencies below 400 Hz. The energy dissipation ratio then dropped with increasing frequency to roughly 50% at 2 kHz. This indicates that different impact velocities generated different densification states in the silicone foam and, therefore, the energy dissipation ratio was reduced. The frequency-domain energy dissipation ratio can be compared with the time-domain energy dissipation shown in Table 2. A total

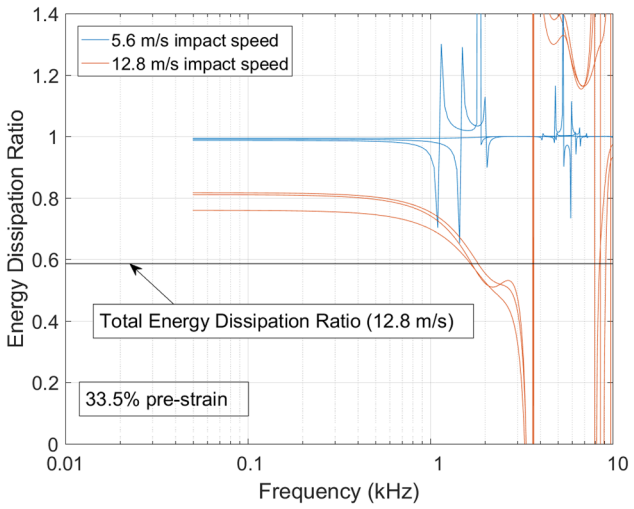

Fig. 7 Energy dissipation ratio for 33.5% pre-strain samples at two velocities

energy dissipation ratio of 0.5865 (Table 2) was calculated in the time-domain analysis (Eq. 2). In the frequency domain analysis, this energy dissipation ratio was apparently not uniformly distributed to all frequencies. Instead, more energy than the total ratio of 0.5865 was dissipated at low frequencies below 1.5 kHz and less energy than the total ratio of 0.5865 was dissipated at higher frequencies than 1.5 kHz.

Although the time-domain stress histories of silicone rubber and foam were similar under some conditions, the energy dissipation behavior of silicone rubber does not resemble the energy dissipation behavior of silicone foam, as shown in Fig. 8. The low-frequency energy dissipation ratio for silicone rubber ranged from 0.2 to 0.38 at different speeds, which was not sensitive to impact velocity. Overall, the energy dissipation ratio of the silicone rubber was not uniformly distributed over the entire frequency range. The energy dissipation ratio for the silicone rubber seemed to be uniformly distributed over frequencies below 1 kHz, and slightly increased to approximately 0.3–0.42 at frequencies of approximately 3 kHz. The energy dissipation ratio then decreased with increasing frequency.

Figure 9 shows energy dissipation ratio behavior for silicone foam and rubber at individual frequencies of 100 Hz, 500 Hz, and 1000 Hz for all experiments. Overall, the behavior is similar to the total energy dissipation ratio-final density behavior shown in Fig. 6. However, the behavior at different frequencies is a bit different compared to the total energy dissipation ratio. For example, the data points at approximately 1350 kg/m^3 at 12.8 m/s speed show a slightly decreasing energy dissipation ratio when frequency increased from 100 to 1000 Hz. This decrease in energy dissipation ratio with increasing frequency seems to be limited to the critical density range from 1200 to 1400 kg/m^3; above and below this density range the energy dissipation ratios from 100 to 1000 Hz are nearly identical. This information can be used to determine foam pre-strain in shock mitigation applications based on energy dissipation/transmission requirements at different frequencies.

Conclusion

A Kolsky compression bar was used to characterize the shock mitigation response of silicone foam and rubber. Silicone foam samples were subjected to various levels of pre-strain and impacted at higher velocities than in a similar

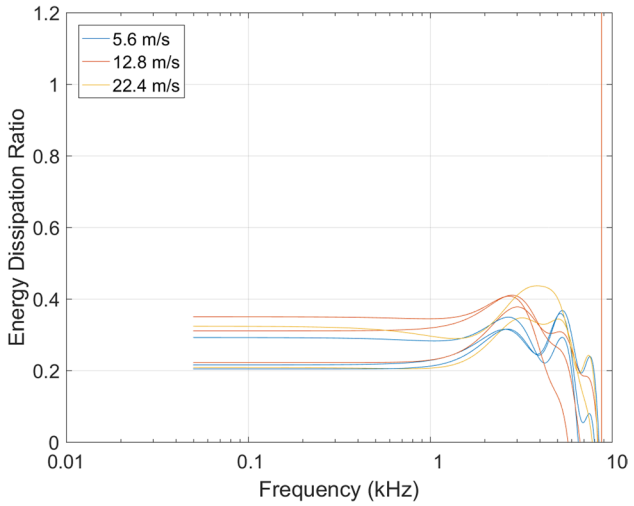

Fig. 8 Energy dissipation behavior of silicone rubber at three different impact velocities

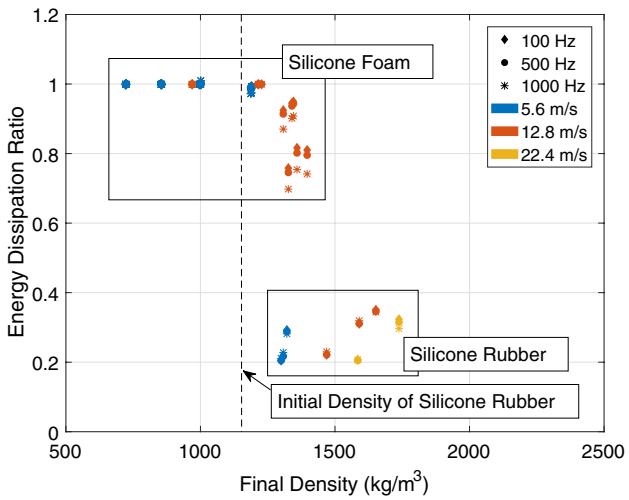

Fig. 9 Energy dissipation ratio at different frequencies and impact velocities for silicone foam and rubber as a function of final density

previous study. Silicone foam was found to be an excellent dissipator of impact energy. At 5.6 m/s impact speed, regardless of pre-strain, the silicone foam dissipated nearly 100% of the impact energy. When the impact speed was increased to 12.8 m/s, the silicone foam dissipated nearly 100% of the impact energy at small pre-strains, but as the pre-strain was increased, the energy dissipation ratio dropped to as low as 0.59 on average. The total energy dissipation ratio for silicone rubber was approximately 0.25, meaning that approximately 75% of the impact energy was transmitted through the material. In the frequency domain, the low-frequency energy dissipated by silicone rubber ranged from 0.2 to 0.38, indicating that at low-frequency energy was transmitted more compared to higher frequency energy. No relationship between impact velocity and low-frequency energy dissipation was apparent for the silicone rubber.

This work suggests that densification state of the foam is a driving factor for increasing energy dissipation capability in silicone-based rubbers and foams. A relationship between energy dissipation ratio and final density of the specimen was found. A critical density of approximately 1200–1400 kg/m^3 was discovered where below that density, the silicone foam dissipated nearly 100% of the energy, regardless of impact speed. When specimen densities higher than 1200–1400 kg/m^3 were reached, the energy dissipation ratio began to decrease, suggesting that if higher foam density was achieved by either higher pre-strain or higher dynamic strain during loading, the energy dissipation ratio would approach that of silicone rubber, or approximately 0.25. This relationship between energy dissipation ratio and final density may be used as a guideline for design in new systems.

Acknowledgements Sandia National Laboratories is a multimission laboratory managed and operated by National Technology and Engineering Solutions of Sandia, LLC., a wholly owned subsidiary of Honeywell International, Inc., for the U.S. Department of Energy's National Nuclear Security Administration under contract DE-NA-0003525. The views expressed in the article do not necessarily represent the views of the U.S. Department of Energy or the United States Government.

References

1. Zhou CY, Yu TX (2009) Analytical models for shock isolation of typical components in portable electronics. Int J Impact Eng 36:1377–1384. https://doi.org/10.1016/j.ijimpeng.2009.03.013
2. Benning CJ (1969) Effect of cell structures in polyethylene foam on shock mitigation. J Cell Plast 5(1):40–45. https://doi.org/10.1177/0021955x6900500105
3. Zhang Z, Ming F, Zhang A (2014) Damage characteristics of coated cylindrical shells subjected to underwater contact explosion. Shock Vib 2014:764607 1–15. https://doi.org/10.1155/2014/763607
4. Rabe JA, Spells S, Rasch DM, Homan GR, Lee CL (1981) Evaluation of silicone foam for flat plate solar collector insulation. Sol Energ Mater 4:159–168. https://doi.org/10.1016/0165-1633(81)90039-3
5. Blood RP, Ploger JD, Yost MG, Ching RP, Johnson PW (2010) Whole body vibration exposures in metropolitan bus drivers: a comparison of three seats. J Sound Vib 329:109–120. https://doi.org/10.1016/j.jsv.2009.08.030
6. Hu WJ, Huang XC, Fan ZG, Si PG (2014) A phenomenological constitutive model for silicone foam under large deformations. In: International conference on mechanics and materials engineering (ICMME 2014)
7. Lu WY (2015) Compression of silicone foams. In: Society for experimental mechanics conference. https://doi.org/10.1007/978-3-319-21762-8_27
8. Sanborn B, Song B (2019) Poisson's ratio of a hyperelastic foam under quasi-static and dynamic loading. Int J Impact Eng 123:48–55. https://doi.org/10.1016/j.ijimpeng.2018.06.001
9. Gibson L, Ashby F (1999) Cellular solids: structure and properties, 2nd Edition. Cambridge University Press, Cambridge
10. Song B, Nelson K (2015) Dynamic characterization of frequency response of shock mitigation of a polymethylene diisocyanate (PMDI) based rigid polyurethane foam. Lat Am J Solids Struct 12:1790–1806. https://doi.org/10.1590/1679-78251585
11. Sanborn B, Song B, Smith S (2016) Pre-strain effect on frequency-based impact energy dissipation through a silicone foam pad for shock mitigation. J Dyn Behav Mater 2:138–145. https://doi.org/10.1007/s40870-015-0043-1
12. Sanborn B, Song B, Nishida E, Knight M (2017) Experimental evaluation of a low-pass shock isolation performance of elastomers using frequency-based Kolsky bar analyses. Lat Am J Solids Struct 14(3):560–574. https://doi.org/10.1007/s40870-015-0043-1
13. Nie X, Song B, Loeffler CM (2015) A novel splitting-beam laser extensometer technique for Kolsky tension bar experiment. J Dyn Behav Mater 1:70–74. https://doi.org/10.1007/s40870-015-0005-7
14. Beccu B, Lundberg B (1987) Transmission and dissipation of stress wave energy at a percussive drill rod joint. Int J Impact Eng 6(3):157–173. https://doi.org/10.1016/0734-743X(87)90019-4
15. Song B, Chen W (2006) Energy for specimen deformation in a split Hopkinson pressure bar experiment. Exp Mech 46:407–410. https://doi.org/10.1007/s11340-006-6420-x
16. Chen W, Song B (2011) Split Hopkinson (Kolsky) bar. Design, testing and applications. Springer, New York, pp 217–219. https://doi.org/10.1007/978-1-4419-7982-7_6